Standoff CW Radar for Through-the-Wall Detection of Human Heartbeat Signatures

Vincent R. Radzicki
Dept. of Elec. and Comp. Eng.
University of California,
Santa Barbara
vradzicki@umail.ucsb.edu

David Boutte
Akela Inc.
Santa Barbara, CA 93111
dboutte@akelainc.com

Paul V. Taylor
Akela Inc.
Santa Barbara, CA 93111
pvtaylor@akelainc.com

Hua Lee
Dept. of Elec. and Comp. Eng.
University of California,
Santa Barbara
hualee@ece.ucsb.edu

***Abstract*—The design and development of a personnel radar detection system based on the identification of micro-Doppler shifts from heartbeat motion is presented here. The paper reviews the phenomenon of micro-Doppler effects measured in radar systems, and describes a specific detection scheme based on this theory. The detection performance for a general radar system is described, and specific results for a prototype system are then presented and analyzed in support of the theory. The signal processing techniques used to estimate heartbeat rates are described in detail and experimental results are provided for actual human targets demonstrating the effectiveness of the system design. The results focus on the detection capability as a function of standoff range to provide a real-world performance measure of the system.**

I. Introduction

Radar detection of human targets has become an increasingly important area of study in the field of radar technology. The ability of radar signals to penetrate buildings, concrete, rubble, and other optically opaque materials allows for the detection of people in unknown and unseen environments[1,2]. This provides advantages over other personnel detecting technologies such as infrared and optical camera systems.

Classical radar systems designed to locate large metallic targets such as planes and vehicles are ill-suited for the detection of people, which are targets with relatively low radar-cross section (RCS). The motion of a person can be detected through Doppler shifts induced on the radar waveform, and human physiological motion, specifically heartbeat motion, has a high-degree of uniqueness providing a strong discrimintating feature for identification tasks that compensates for their low RCS [3,4]. The Doppler shift resultant from small-scale movements of the target structure has been referred to as the micro-Doppler effect in the literature and has provided new techniques for modelling radar targets[5].

A portable, standoff radar system is presented for detection of human targets in through-the-wall scenarios. The system operates in continuous wave (CW) mode and performs the detection task through measurement of the micro-Doppler reflections and subsequent processing to identify unique heartbeat signatures. Applications would have impact in search-and-rescue missions, military operations, and law-enforcement. Advancements in this field have been made for medical applications of radar sensing, however, these technologies have been more focused on detection ranges much closer than desired for adequate standoff radar performance[6]. A description of the model used to describe human radar reflections is first described, followed by an estimation procedure for detecting the presence of a human, and lastly the experimental results are discussed.

II. Model of Human Radar Signals

The micro-Doppler signautures generated from a target under radar illumination is directly related to its motion. Therefore, characterizing the type of motion the target follows is key to understanding and interpreting the micro-Doppler components present in the received signals. The prior work on modelling of human motion under radar illumination is extensive, and much of the modelling utilizes the concept of the micro-Doppler phenomenom introduced earlier [7,8,9]. One specific type of motion that has been of interest is the periodic nature exhibited by a person's heartbeat and breathing patterns. A brief overview of the phenomenon is presented here.

Given a monostatic radar system illuminating a target with a CW waveform, the transmit signal can be written as

$$e_T(t) = A_T e^{j2\pi f_c t} \tag{1}$$

where f_c is the carrier frequency and A_T is the amplitude of the waveform. If the transmit signal is reflected from a single target, the received signal will be a scaled and phase-shifted version. If the target is at a time-varying range from the transceiver $r(t)$, the corresponding phase shift at the receiver will also be a time varying function $\Delta\theta(t)$. The corresponding received signal will be in the form

$$\begin{aligned} e_R(t) &= A_T A_R e^{j(2\pi f_c t - \Delta\theta(t))} \\ &= A_T A_R e^{j(2\pi f_c t - 2\pi \frac{2r(t)}{\lambda})} \end{aligned} \tag{2}$$

The terms A_R and λ are the signal attenuation factor and wavelength respectively, and the doubling factor of the range is due to the two way propagation of the waveform.

This model may be extended to describe mutliple targets by superimposing their mutltiple reflections at the received signal. For human detection scenarios, the two main oscillating targets of interest are the chest cavity undergoing breathing

978-1-5090-0863-6/16/$31.00 ©2016 IEEE

and the heart. Due to the proximity of both of these targets and complex structure they share, simply superimposing the relfections may not always be accurate. However, to simplify the complexity of the analysis and signal processing, the focus for the rest of the paper will be on the heartbeat structure alone assuming that it is an independent isolated target. The periodic motion of the heartbeat can thus be described within this framework, and the corresponding Doppler shift can be formulated.

Let the range position of the target from the radar be expressed as:

$$r_p(t) = r_0 - r_A \sin(2\pi f_h t) \tag{3}$$

where r_A is the maximum offset from the equilibrium position of the target and f_h is the frequency of oscillation of the heartbeat. The received signal in this case will be

$$\begin{aligned} e_R(t) &= A_T A_R e^{j(2\pi f_c t - 2\pi \frac{2r_p(t)}{\lambda})} \\ &= A_T A_R e^{j(2\pi f_c t + \frac{4\pi r_A}{\lambda}\sin(2\pi f_h t) - \frac{4\pi r_0}{\lambda})} \end{aligned} \tag{4}$$

Demodulation of the received signal with the original transmit signal to isolate the time-varying Doppler component yields

$$\begin{aligned} x_D(t) &= e_T^H(t) e_R(t) \\ &= E e^{j\frac{4\pi r_A}{\lambda}\sin(2\pi f_h t)} \end{aligned} \tag{5}$$

where $E = A_R A_T^2 e^{j\frac{-4\pi r_0}{\lambda}}$ is a constant complex scalar. The demodulated Doppler component will therefore be of constant amplitude and have a sinusoidally varying phase component as presented in (5). This model implies the received signal will have a periodic nature, which can be used for identificatin purposes. This signal model has also been shown to be an accurate description of radar propagation in through-the-wall scenarios [10]. Sections III and IV describe in more detail how to use this information for human detection in standoff through-the-wall scenarios.

III. Detection of Heartbeat Doppler Signatures

The micro-Doppler signal described in (5) contains a time-varying frequency component in contrast to typical sinusoidal signals. To describe time-vary spectral information, the notion of an instantaneous frequency has been developed[11]. The instantaneous frequency of a signal is defined as the time-derivative of its phase

$$f(t) = \frac{1}{2\pi}\frac{d}{dt}\theta(t) \tag{6}$$

For constant frequency signals, it can be shown that its phase changes linearly over time. Referring to the micro-Doppler signal in (5), the Doppler induced phase-shift of a heartbeat signal varies sinusoidally in time.

$$\theta_D(t) = 2\pi \frac{r_A \sin(2\pi f_h t)}{\lambda} \tag{7}$$

Classical Fourier analysis is ill-suited for estimating the instantaneous frequency component as no time information is preserved. The short-time Fourier transfrom (STFT) is a well-known time-frequency transformation for analyzing time-varying spectral information. The STFT of the signal $x_D(t)$ can be used to estimate the Doppler-shift of the signal over a small window in time. It is computed by taking a Fourier transform of each windowed segment, which can be expressed mathematically as

$$X(\tau, f_D) = \int x_D(t) w(t-\tau) e^{-j2\pi f_D t} dt \tag{8}$$

where $w(t)$ is the windowing function that serves to select the segements of $x_D(t)$, the time τ is the start time of the windowed segment, and f_D refers to the Doppler shift at each window position. The STFT is usually visualized in log-magnitude form $X_{dB}(\tau, f_D) = 10\log_{10}|X_{dB}(\tau, f_D)|^2$, typically referred to as a spectrogram.

Letting the window function be of length L, a single segment of the micro-Doppler signal at window time τ from (5) may be written as

$$x_D(t)w(t-\tau) = \begin{cases} E e^{j\theta_D(t)} & ,\tau < t < \tau + L \\ 0 & ,otherwise \end{cases}$$

where $\theta_D(t)$ is the signal's phase-Doppler over the window length. If the window length is chosen such that it is a fraction of the period of the heartbeat oscillation $T_h = \frac{1}{f_h}$, the phase change over this small time period can be approximated as linear so that the frequency is then a constant doppler shift f_{D_0}.

$$\begin{aligned} f_D(t) =& \frac{1}{2\pi}\frac{d}{dt}\theta_D(t) && L << T_h \\ =& \frac{d}{dt}\frac{r_A \sin(2\pi f_h t)}{\lambda} \\ \approx& f_{D_0} \end{aligned} \tag{9}$$

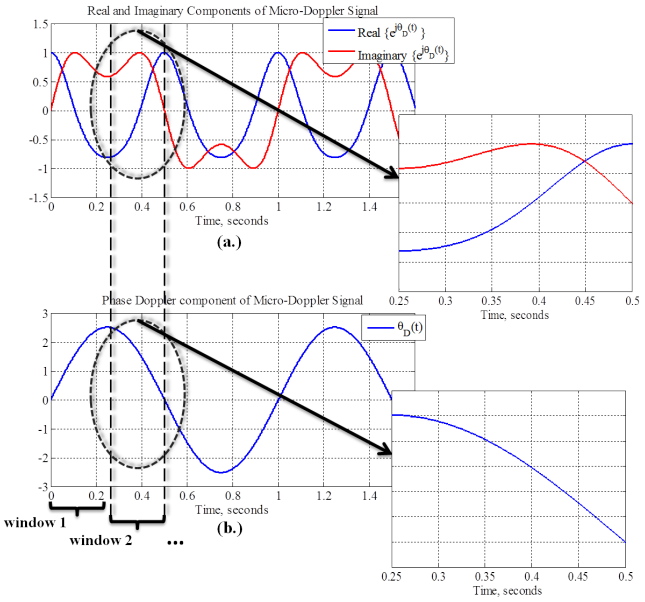

Fig. 1. (a.) The micro-Doppler heartbeat signal and (b.) Doppler-induced phase component.

To illustrate this concept, the micro-Doppler signal in equation (5) was simulated where the frequency of oscillation of the heartbeat was defined to be $f_h = 1Hz$ and the maximal range displacement was set to $r_A = 1cm$. Figure 1 shows the micro-Doppler signal $x_D(t)$ over time and its corresponding phase-Doppler component $\theta_D(t)$, as well as an enlarged portion of a windowed segment. Over the course of the entire signal, it clearly does not have linear phase. However, over a small portion of one period of oscillation the phase may be viewed as approximately linear, as was stated in equation (9). This approximation becomes less accurate around the maxima and minima of the phase function as the derivative approaches zero at these times. For the windowed segments not around these points, the linear phase approximation means that the instantaneous spectrum of that window will contain only one dominat peak similar to a CW waveform. Figure 2 displays the spectrogram of the simulated micro-Doppler signal, along with an outline of the true instantenous frequency. Note how the spectrogram in most regions is comprised of a single peak that accurately tracks the instantenous Doppler frequency as predicted from the approximation.

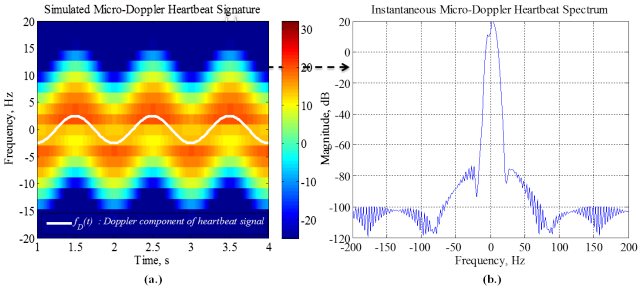

Fig. 2. (a.) Spectrogram of Simulated micro-Doppler Heartbeat Signature and (b.) Instantaneous spectrum around 3.5 seconds.

The model developed up to now serves as a useful tool for analyzing the spectral content of micro-Doppler signals over time. For real-world Doppler radar measurements, the heartbeat micro-Doppler signal will be extremely small and not the dominant component of any measured spectrogram. To detect the heartbeat signals presenece, however, we have shown that the instantenous freqeuncy component will vary periodically over time. The more dominant Doppler signals present in radar measurements typically do not display this periodic behavoir. This means that isolating the periodically varying Doppler components in the spectrogram, can signify the presenece of a heartbeat target.

By taking a second Fourier transform of the STFT spectrogram $|X_{dB}(\tau, f_D)|$ over the window time τ, the time-varying nature of each Doppler component can be characterized. This procedure may be expressed as

$$\hat{X}(f_v, f_D) = \mathscr{F}_\tau\{|X_{dB}(\tau, f)|\} \tag{10}$$

where now f_v is the frequency of oscillation for each Doppler componet f_D. This second transformation was performed on the simulated heartbeat signal spectrogram, and the corresponding profile can be seen in Fig. 3. The periodic spectrum

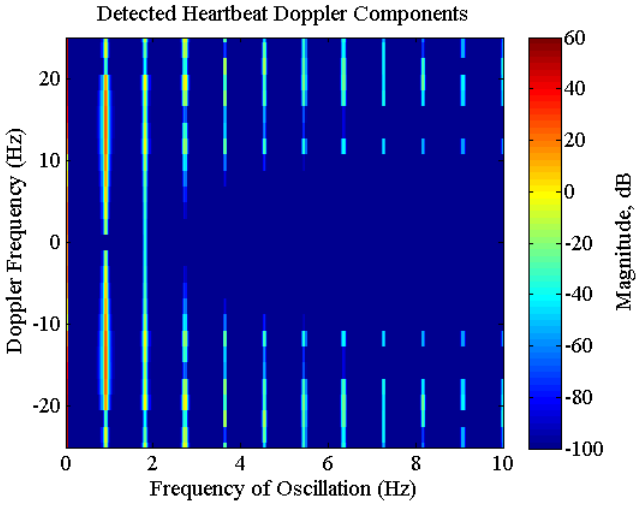

Fig. 3. Simulated estimate of micro-Doppler heartbeat frequency of oscillation

of the heartbeat signal contains a main peak occuring at the frequency of oscillation ($f_H = 1Hz$), followed by smaller peaks corresponding to the higher order harmonics.

With the theoretical tools in place for heartbeat detection, to attain a performance estimate of the radar system the expected probability of detection (P_d) vs. signal-to-noise ratio (SNR) should be calculated, typically referred to as the receiver operating curve (ROC). For a given probability of false alarm (P_{fa}), the ROC of a radar detecting a single CW frequency in the presence of additive white gaussian noise (AWGN) utilizing a quadrature receiver with an envelope detector has been derived analytically [12]. This ROC can serve as an upper-bound performance benchmark for the detection of micro-Doppler heartbeat signals, as the heartbeat detection was approximated as estimating a single frequency over a short-time window [13,14]. If the SNR for a particular radar system remains constant over each time-window, one can expect similar performance to that displayed in the specific ROC shown in Fig. 4.

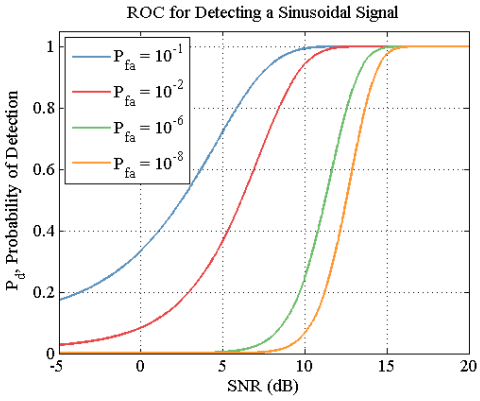

Fig. 4. ROC for Radar Dectection of a Sine Wave

Successful detection of the heartbeat signal requires both sufficient SNR, as well as an estimate of the heartbeat's rate

or frequency of oscillation ($\hat{f}_h$). For a modern radar system system much of the processing is done using digital signal processing on sampled data from the received signal $x_D(t)$. The analysis up to here, has an analgous form in the discrete domain that can be applied to the sampled Doppler data $x_D(n)$. The discrete STFT can be found by peforming an N-point DFT on each windowed segment of the data.

$$X(m,k) = \sum_{n=0}^{N-1} x_D(n-m)w(n)e^{-j\frac{2pikn}{N}} \tag{11}$$

The second Fourier transform of the spectrogram may then be implemented with another DFT computed over the window index m.

$$\hat{X}(l,k) = DFT_m\{|X_{dB}(m,k)|\} \tag{12}$$

Here k refers to the f_k DFT frequency bin of the original doppler shift f_D, and l refers to the f_l DFT frequency bin for the oscillation frequency (f_v). The discrete processing presented here, was used to estimate the heartbeat oscillation frequency for the experimental data presented next.

IV. Experiments and Results

A set of experiments were conducted with a prototype AKELA CW Radar system to explore the model presented thus far and test the system's detection capability for through-the-wall scenarios of human targets. Most importantly, the system was tested at different standoff ranges, to determine and quantify the maximal detectable range. All data processing was done in the MATLAB programming enviornment.

A. Hardware

The experimental system used for data collection was designed from previous Akela radar technology optimized for the measurement of small phase changes reflected from low-RCS targets. The antenna array was comprised of a single bi-static pair and a homodyne architecture was employed as the receiver by directly down-converting to baseband. A system block diagram along with a photo of the prototype can be seen in Fig. 5.

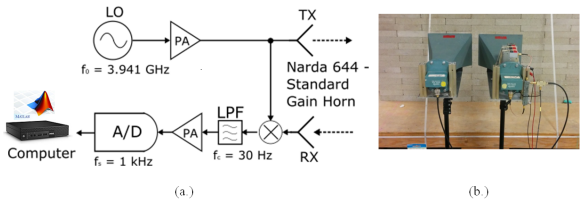

Fig. 5. (a.) Hardware System Diagram and (b.) Prototype Hardware

A stable, low-noise local oscillator (LO) was used to generate the single CW sinusiod waveform that was inserted into a two-way power splitter, where one portion of the signal was directed to the transmit antenna and the other to the mixer. The transmit and receiver antennas were both standard gain horns with boresight gains of $16dB$. The received signal was demodulated directly to baseband through the mixer and the low-pass filter (LPF) removed the HF components and noise. The demodulated and low-passed signal would contain the reflected Doppler information as presented in the previous analysis. Lastly, this signal was then sampled and stored for further processing by a desktop computer.

TABLE I
Hardware Parameters

Transmit Frequency	3.941 (GHz)
Transmit Power	18 (dBm)
Sampling Rate	1 (kHz)
Antenna Boresight Gain	16 (dB)
Low Pass Cutoff Frequency	30 (Hz)

A summary of the hardware parameters discussed are listed in Table 1. One key parameter, is the transmit frequency to use as the probing waveform. Using a higher frequency signal is desirable so that the small movements of a heartbeat will induced a larger phase shift relative to the wavelength. However, utilizing high-frequency bands such as X-band or higher will not have as great penetrating depths as lower frequency bands. Given the small-phase measurements required, another key design factor to take into consideration is the phase-noise and stability of the oscillator.

B. Experiment Design

The set of experiments were conducted in an indoor, controlled lab setting for repeatibility. A concrete wall $19cm$ thick was built for testing purposes, and a single person was designated as the target for all testing. The radar system and human were situated on opposite sides of the wall, where the target was placed at a specific offset distance (d_T) from the radar. A diagram of the experiment scenario can be seen in Fig. 6, along with a photo of the experimental setup. For each data

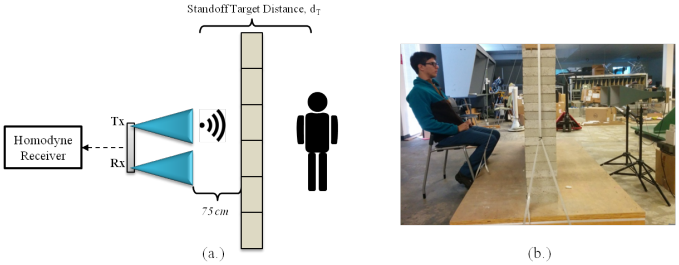

Fig. 6. (a.) Experimental Diagram and (b.) setup

set, the target sat in a stationary position and was illuminated for a total observation time of $120s$ by the radar system while data was collected. The antennas were placed $75cm$ back from the wall, and the target was positioned at the nominal ranges of $d_T = 1.75m, 2.25m, 2.75m, 3.25m, 3.75m$. A control data set was recorded with no target present to estimate the noise and interference.

C. Results

The data was processed using the detection algorithm presented in Section II. The window length for the STFT

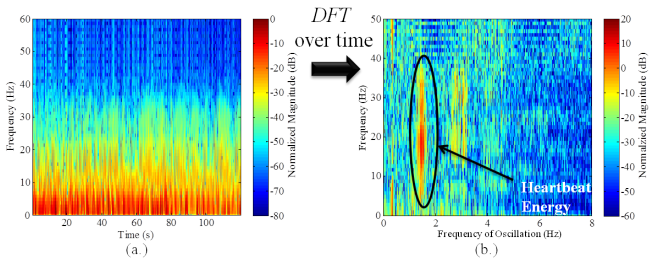

Fig. 7. (a.) Spectrogram of heartbeat's micro-Doppler signal (b.) 2-D DFT of heartbeat's micro-Doppler

was set to be $L = 0.256$ seconds, so that the linear-phase approximation at each window would be valid. The window overlap percentage was set to 87.5%. For the target position at $d_T = 1.75m$, both the spectrogram and 2-D DFT were computed and displayed in Fig. 7. As can be seen in the spectrogram, the spectral values below $5Hz$ are dominated by the phase noise of the oscillator, however, above this band small variations in the spectrum across time are present. The variations are more easily seen by looking at the frequency of oscillations in the 2-D DFT. Most of the oscillation energy is located around $1.5Hz$ or about 90 beats per minute (BPM), a typical heartbeat rate.

The mean oscillation energy in the 2D DFT, was then computed by averaging the osciallation energy over all the Doppler frequencies in the spectrogram for each data set. The results of this computation are plotted in Fig. 8 along with the background measrument for comparison. The frequency $\hat{f}_h$ where most of the energy is located in the averaged spectrum should correspond to the estimate of the target's heartbeat rate. As is seen in Fig. 4 (a-c), the heartbeat estimate varies between $1.4Hz - 1.6Hz$ or $84-96$ BPM for the target up to a distance of $d_T = 2.75m$. For the first data set, notice a smaller but visible peak exists at an oscillation of $\hat{f}_B = 0.25Hz$. This peak is most likely a result of the periodic movement of the chest cavity of the target. The heartrate estimate is reasonably close to typical heartbeat rates for an adult person. However, as can be seen in Fig. 8-(d) beyond this distance, there is no discernible peak in the spectrum leaving the heartrate estimation difficult. By setting an appropriate threshold above the noise-floor for this measurement, a decision can be made if a human target is present along with an estimate of the target's heartbeat.

To quantify the measurement accuracy the SNR was calculated at each standoff distance. The signal power can be estimated by integrating the power spectral density (PSD) over the band of operation. As observed earlier, the phase noise component up to $5Hz$ is dominat. The band for computing the power measurements was restricted from $5Hz$ up to the LPF cutoff frequency of $30Hz$.

For estimating the total noise power present the background control data set was used, and to estimate signal power the data set at each standoff range was used. The instantaneous PSD at each short-time window was integrated and the final power

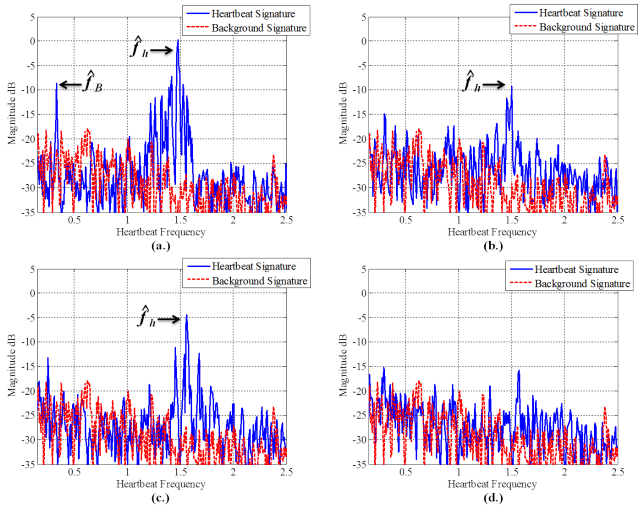

Fig. 8. Heartbeat estimation for human target at (a.) $d_T = 1.75m$ (b.) $d_T = 2.25m$ (c.) $d_T = 2.75m$ (d.) $d_T = 3.25m$

measurement was taken as the average over all time. The subsequent ratio between the two was found, and the resultant SNR vs. stand-off range can be seen in Fig. 9. The expected signal attenuation due only to path loss was also calculated using the basic radar equation and plotted for comparison.

At the closest standoff ranges the SNR is about $8dB$, and according to the ROC from Section II that should yield a relatively high P_d for P_{fa} values of 10^{-1}, 10^{-2}. At the standoff ranges $2.5m$ to $3m$ the SNR drops off to almost $0dB$ and therefore would yield a very low P_d. These observations support the maximum detectable range determined through the heartbeat estimation procedure performed earlier, and also demonstrate the performance limitations for this experimental setup.

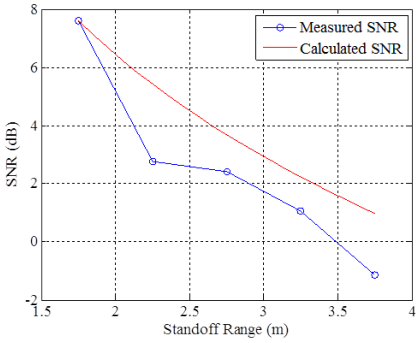

Fig. 9. SNR vs. Range of Human Target

V. Conclusions

An overview of the theory that the detection scheme was based on was discussed, followed by a typical performance bound for a general radar system. Next, the experiment design used to test the theory was described along with the results. A key takeaway from the experiments was the limiting factor

in the radar system was the oscillator's phase noise which made detecting the heartbeat signal presented in the theory difficult. Also, other factors beyond the designer's control such as non-stationary clutter in the environment also can limit performance. It was shown that by limitng the target to an offset distance of $< 3.0m$, detection and estimation of the heartbeat rate is achievable.

Potential improvements to the current model include incorporating moving targets to determine the effects on the heartbeat micro-Doppler componets. Also, extending the system to wide-band modalities such as Frequency Modulated Continuous Wave (FMCW) will allow for both detection and ranging of targets. This capability greatly increases the potential applications of the technology. By providing the experimental parameters used to achieve the results presented here, it will be the focus of future work to build a more complete model and toolset for the detection of heartbeat signals so that radar engineers may design and build personnel detection radar systems in a more robust manner.

ACKNOWLEDGMENT

This research was supported by Akela Inc. and the Imaging Systems Labratory at University of California, Santa Barbara.

REFERENCES

[1] A. .S Bugaev; V. V. Chapursky; S. .I. Ivashov; V. V. Razevig; A. P. Sheyko; I. A. Vasilyev, "Through wall sensing of human breathing and heart beating by monochromatic radar," in *Ground Penetrating Radar, 2004. GPR 2004. Proceedings of the Tenth International Conference on* , vol.1, no., pp.291-294, 21-24 June 2004

[2] M. D'Urso; F. Gianota; R. Lalli; L. Infante, "Differential approach for Through-the-wall life signs detection," in *Radar Conference, 2010 IEEE* , vol., no., pp.1079-1082, 10-14 May 2010

[3] A. S. Bugaev; et al., "Radar Methods of Detection of Human Breathing and Heartbeat", *Journal of Communications Technology and Electronics*, vo. 51, no. 10, 2006, pp. 1154-1168

[4] D. Tahmoush; J. Silvious, "Radar micro-doppler for long range front-view gait recognition," in *Biometrics: Theory, Applications, and Systems, 2009. BTAS '09. IEEE 3rd International Conference on* , pp.1-6 2009

[5] V .C. Chen; et al., "Radar Micro-Doppler Signatures for Characterization of Human Motion," in Chapter 15 *Through-the-Wall Radar Imaging* , M.Amin, (ed.), Boca Raton, FL: CRC Press, 2010

[6] J. Kranjec, S. Begus, J. Drnovsek and G. Gersak, "Novel Methods for Noncontact Heart Rate Measurement: A Feasibility Study," in IEEE Transactions on Instrumentation and Measurement, vol. 63, no. 4, pp. 838-847, April 2014.

[7] V .C. Chen, *The Micro-Doppler Effect in Radar* , 1st ed, Norwod, MA: ARTECH HOUSE

[8] V .C. Chen; Fayin Li; S.S. Ho; H. Wechsler, "Micro-Doppler effect in radar: phenomenon, model, and simulation study," in *Aerospace and Electronic Systems, IEEE Transactions on* , vol.42, no.1, pp.2-21, 2006

[9] P. Setlur; M. Amin; T. Thayaparan, "Micro-doppler signal estimation for vibrating and rotating targets," in *Signal Processing and Its Applications, 2005. Proceedings of the Eighth International Symposium on* vol.2, no., pp.639-642, August 28-31, 2005

[10] X. Liu; H. Leung; G. A. Lampropoulos; "Effects of Non-Uniform Motion in Through-the-Wall SAR Imaging," in *IEEE Transactions on Antennas and Propagation* vol.57, no.11, pp.3539-3548, 2009

[11] B. , Boashash, "Estimating and interpreting the instantaneous frequency of a signal. II. Algorithms and applications," in *Proceedings of the IEEE* , vol.80, no.4, pp.540-568, Apr 1992

[12] A. D. Whalen, *Detection of Signals in Noise*, pp. 103, 1st ed., New York, NY: ACADEMIC PRESS

[13] Xiang-Gen Xia; Genyuan Wang; Chen, V.C., "Quantitative SNR analysis for ISAR imaging using joint time-frequency analysis-Short time Fourier transform," in *Aerospace and Electronic Systems, IEEE Transactions on* , vol.38, no.2, pp.649-659, Apr 2002

[14] M. Anderson; "Design of multiple frequency continuous wave radar hardware and micro-Doppler based detection and classification algorithms", PhD Dissertation, Dept. Elect.and Comp. Eng., UT, Austin, TX, 2008